Growth of 3,4,9,10-perylenetetracarboxylic-dianhydride crystallites on noble metal surfaces

Th. Wagner *, A. Bannani, C. Bobisch, H. Karacuban,
M. Stöhr, M. Gabriel, R. Möller

Fachbereich Physik, University of Duisburg-Essen, Universitätsstraße 5, D-45117 Essen, Germany

Abstract

The growth of organic crystallites formed by 3,4,9,10-perylenetetracarboxylic-dianhydride (PTCDA) has been investigated by scanning tunneling microscopy on Cu(1 1 0), Cu(1 1 1) and Au(1 1 1). For the chosen parameters PTCDA exhibits Stranski–Krastanov growth. If the average coverage exceeds about 3–5 monolayers the formation of crystalline islands begins. Working at very low tunneling currents it has been possible to obtain molecular resolved images of crystallites formed by up to 100 molecular layers, while the overall coverage has a value of about 10–20 monolayers. Since the side walls typically exhibit a moderate slope in the range of 14–20° their structure may be as well analyzed as the flat top layer. As will be presented it is not only possible to determine the unit cell within the molecular layer but also their relative displacement between subsequent layers. A comparison between the 3D structures of several crystals will be given.
© 2004 Elsevier B.V. All rights reserved.

1. Introduction

In view of potential application in molecular electronics and optoelectronics various organic molecules are currently of interest. Some combinations (e.g. of 3,4,9,10-perylenetetra-carboxylic-dianhydride (PTCDA) and copper-phthalocyanine) are already in use for organic light emitting diodes. To realize an electronic device two interfaces to inorganic conductors are required. The quality of these interfaces may be crucial to the performance.

Hence, the growth of organic molecules on inorganic surfaces has been the subject of many investigations (see e.g. [1–7]). Epitaxial growth of two planar molecules has been demonstrated by Schmitz-Hübsch et al. [8] for PTCDA on hexa-benzocoronene and by Staub et al. [9] for PTCDA on decanethiol. They also observed the beginning of crystalline growth of a small crystallite, which was tentatively identified as α-type crystal. A coverage of up to 3.5 monolayers has been analyzed by Chizhov et al. [10] for PTCDA on Au(1 1 1). The analysis of the bulk of PTCDA by electron diffraction [11] and [12] revealed two phases (α and β). The growth of crystalline films of PTCDA on Ag(1 1 1) has been analyzed by grazing incidence X-ray diffraction and scanning force microscopy by

* Corresponding author. Tel.: +49-201-183-2470; fax: +49-201-183-3132.
E-mail address: thorsten.wagner@uni-essen.de (Th. Wagner).

Krause et al. [13]. The present paper will focus on the growth of organic crystallites with a height of up to 100 molecular layers. As pointed out in a previous paper [14] the three dimensional structure of the crystallites may be derived from molecular resolved images of the facets.

2. Experimental

The experiments have been performed in an ultra high vacuum system consisting of separate chambers for sample preparation and characterization. The surfaces of single crystals have been prepared by repeated cycles of sputtering (Ar+-ions: 1.4 keV, 10 μA/cm^2) and thermal annealing. The result of this procedure was checked by XPS and by STM. The PTCDA molecules have been evaporated from a small self-built crucible kept at a temperature of 510 K providing a flux of about 2–4 monolayers/min at the sample. Prior to the measurements the flux of particles has been carefully checked by a quadrupole mass spectrometer. For the results presented in this paper the equivalent of 10–20 monolayers has been deposited. The films have been thermally annealed using a linear temperature ramp (1 K/s) ending at a temperature ranging from 510 to 530 K. During the process of the sample preparation the base pressure in the vacuum system was 5×10^{-10} mbar. The base pressure of the STM chamber is 2×10^{-11} mbar. The samples have been transferred in situ to a home built STM, which is optimized to provide minimal electric noise by capacitive pick-up of line frequency etc. In combination with a self built current-to-voltage converter it allows to operate the STM at a tunneling current down to 1 pA using a bandwidth of 30 kHz. For the given experiments a typical current of 2 pA has been used. The STM was calibrated by the investigations of the clean Cu(1 1 0), Cu(1 1 1) and Au(1 1 1) surfaces prior to the measurement of the molecular layers.

3. Results

To illustrate the Stranski–Krastanov-type growth of the crystalline films, Figs. 1–3 display
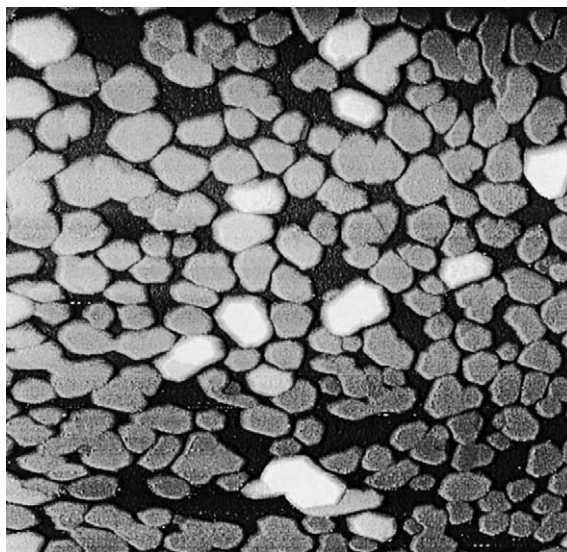

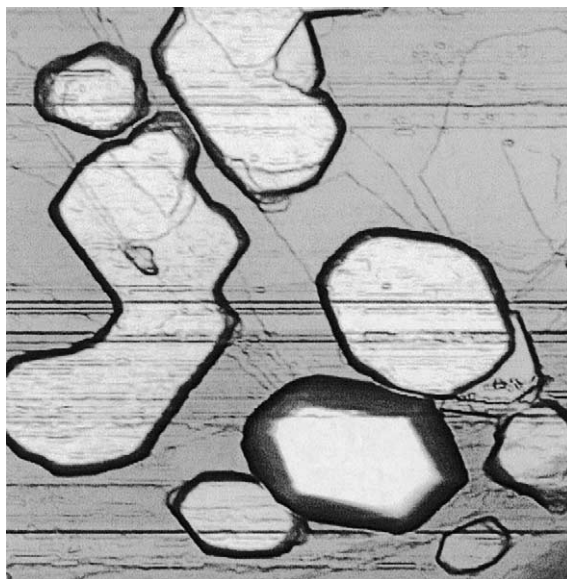Fig. 1. STM-image of a crystalline film of PTCDA on Cu(1 1 0), 1.43×1.35 μm^2 ($U_{tip} = -2.7$ V, $I_t = 1.8$ pA).

Fig. 2. STM-image of a crystalline film of PTCDA on Au(1 1 1), 860×860 nm^2 ($U_{tip} = -2.7$ V, $I_t = 1.0$ pA).

large area scans on Cu(1 1 0), on Cu(1 1 1), and on Au(1 1 1) respectively. It is clearly visible that there is a broad variety in the shape and orientation of the crystallites. In the case of Cu(1 1 0) the height
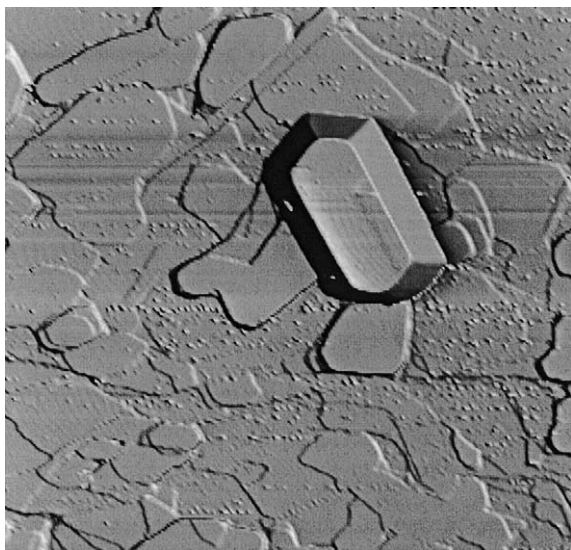
Fig. 3. STM-image of a crystalline film of PTCDA on Cu(1 1 1), 1.4×1.4 μm^2 ($U_{tip} = -2.2$ V, $I_t = 2.0$ pA).

lower height and only a few crystals achieve about twice the lower height. The image on the Au(1 1 1) surface shows that the crystals are surrounded by areas covered by a few ordered monolayers separated by domain boundaries. This was also found for the Cu(1 1 1) surface.

At higher resolution the molecular structure of the crystals becomes visible. The following discussion will focus on six different crystals, three on Cu(1 1 0) (named A, B and C), two on Cu(1 1 1) (named D and E) and one on Au(1 1 1) (named F). For each crystal an overview in combination with detailed images of the top layer and the slopes are displayed in Figs. 4–9.

Given these pictures it is very tempting to deduce the crystalline structure for the different crystals. The analysis is facilitated by the fact that the crystals are formed by layers parallel to the surface. Hence at first the structure within the layers is determined, the displacement between the
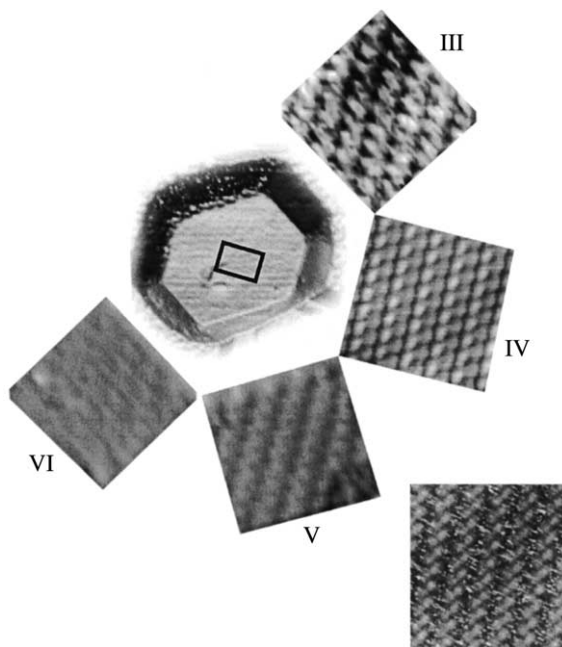
of the crystallites seems to follow a bimodal distribution, as already shown in a previous paper [15]. The majority of the crystals cluster at the
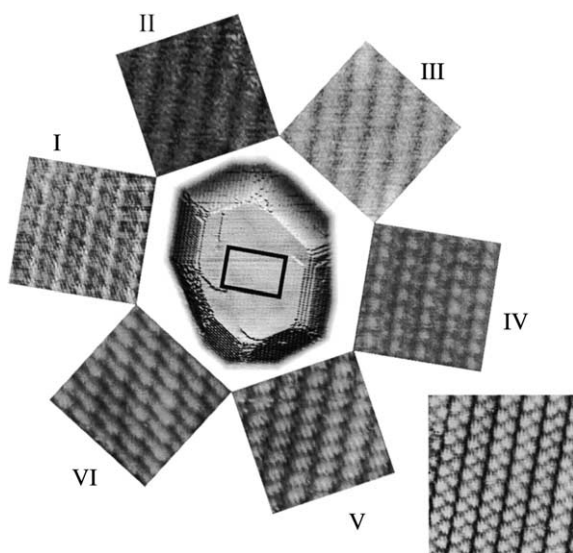
Fig. 4. PTCDA on Cu(1 1 0), STM images of crystallite A, typical imaging conditions $U_{tip} = -3$ V, $I_t = 1.5$ pA, the size of the crystallite is about 100×85 nm^2, the images of the slope labeled from I to VI show areas of about 11×11 nm^2, the image to the lower right displays the top layer, the mean coverage is equivalent to about 20 monolayers.
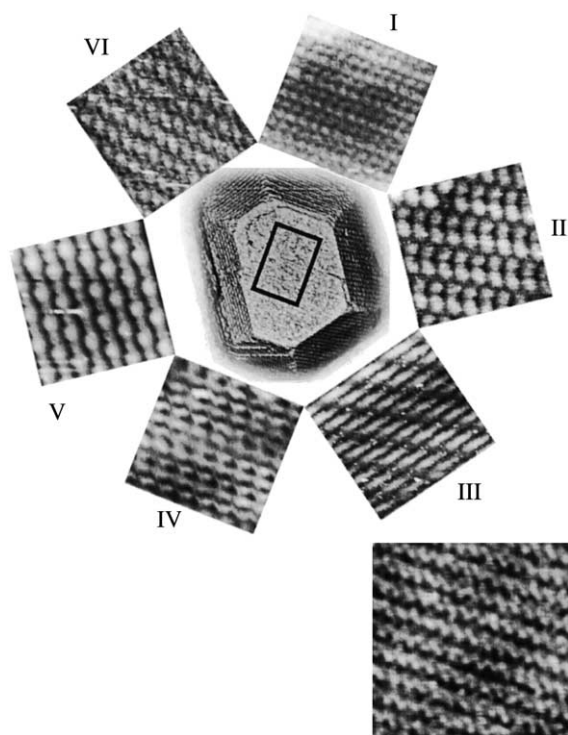

Fig. 5. PTCDA on Cu(1 1 0), STM images of crystallite B, typical imaging conditions $U_{tip} = -2$ V, $I_t = 1.8$ pA, the size of the crystallite is about 120×80 nm^2, the images of the slope labeled from III to VI show areas of about 11×11 nm^2, the image to the lower right displays the top layer, the mean coverage is equivalent to about 20 monolayers.

Fig. 6. PTCDA on Cu(1 1 0), STM images of crystallite C, typical imaging conditions $U_{tip} = -2$ V, $I_t = 1.8$ pA, the size of the crystallite is about 90×75 nm^2, the images of the slope labeled from I to VI show areas of about 11×11 nm^2, the image to the lower right displays the top layer, the mean coverage is equivalent to about 10 monolayers.
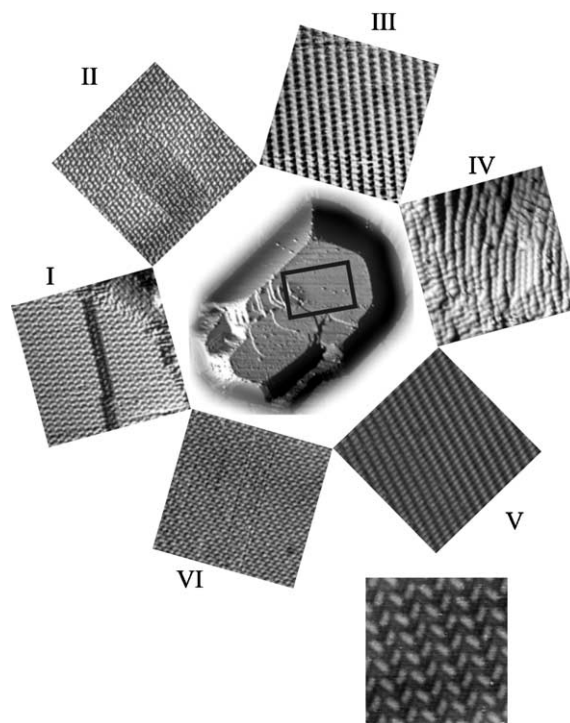

Fig. 7. PTCDA on Cu(1 1 1), STM images of crystallite D, typical imaging conditions $U_{tip} = -3$ V, $I_t = 1.5$ pA, the size of the crystallite is about 550×400 nm^2, the images of the slope labeled from I to VI show areas of about 30×30 nm^2, the image to the lower right displays the top layer, the mean coverage is equivalent to about 10 monolayers.

layers is evaluated in a second step. A close look at the edges reveals that the top layer is not reconstructed. However, a relaxation cannot be excluded.

The highly resolved images of the top layer clearly show that within the experimental errors the unit cell is rectangular. This holds true for all observed crystals. However, there is some variation in the length of the base vectors a (short side) and b (long side), as summarized in Table 1. The arrangement of the molecules within the unit cell is sketched in the lower left corner of Fig. 10. It closely resembles the ordering in the (1 0 2)-plane of the bulk form of PTCDA [12].

Characteristic for all crystallites of PTCDA observed so far is the shape of an irregular hexagon. Two edges are parallel to the short side of the unit cell. The other four are parallel to the diago-

nals. Facets parallel to the long sides of the unit cell have not been observed. Hence the ratio between a and b is reflected in the angles between the edges.

To evaluate the translation between two adjacent layers one may analyze images displaying the top layer with isolated monomolecular steps as shown for crystal D in Fig. 10.

By superposing a scheme of the molecular grid the displacement may be directly determined as indicated by the white lines. For the given figure values of $\Delta a = 0$ Å and $\Delta b = 2$ Å are found. Unfortunately, the procedure may not be applied in general because such a formation has been observed only rarely. Furthermore, the accuracy which may be obtained is rather limited to about 1 Å.

A better evaluation is obtained by a detailed analysis of the slopes of the crystals. The principle of the procedure has been dealt in a previous paper
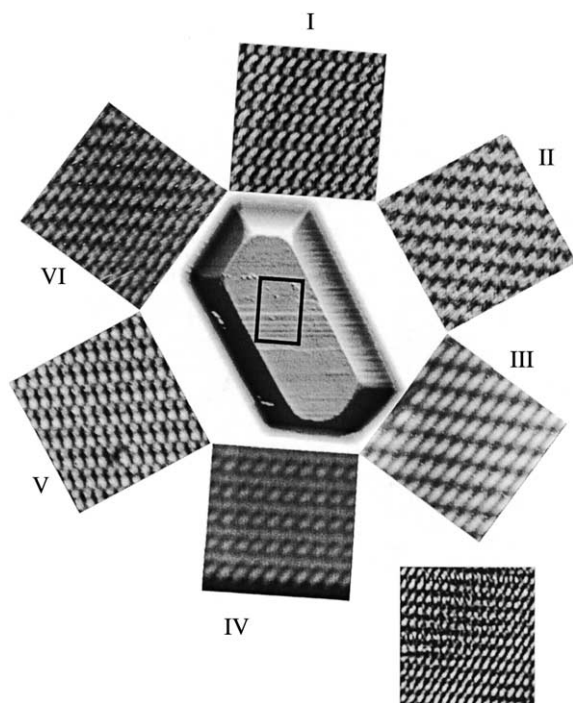
Fig. 8. PTCDA on Cu(1 1 1), STM images of crystallite E, typical imaging conditions $U_{tip} = -3$ V, $I_t = 1.5$ pA, the size of the crystallite is about 650×350 nm^2, the images of the slope labeled from I to VI show areas of about 20×20 nm^2, the image to the lower right displays the top layer, the mean coverage is equivalent to about 10 monolayers.

Fig. 9. PTCDA on Au(1 1 1), STM images of crystallite F, typical imaging conditions $U_{tip} = -3$ V, $I_t = 1.5$ pA, the size of the crystallite is about 390×320 nm^2, the images of the slope labeled from I to VI show areas of about 11×11 nm^2, the image to the lower right displays the top layer, the mean coverage is equivalent to about 10 monolayers.

[14]. In the simplest case, which is no translation at all, features corresponding to equivalent positions in the molecular unit cell for different layers are lined up along the direction of the base vectors of the unit cell. In other words the molecular lattice of the top layer is extended to the slopes. However, the appearance of the unit cell will differ for the different slopes. To illustrate such a situation Fig. 11 displays crystal A with molecular resolution of the top layer and all facets. The white lines indicate the direction of the base vectors of the molecular unit cell of the top layer. Within the experimental errors of about 1° the lines continue in the slope. An equivalent result is obtained by comparing the Fourier transformation of the top layer and the slopes which exhibit the identical reciprocal lattice. It turns out that the crystallites A and B exhibit no displacement between the different molecular layers.
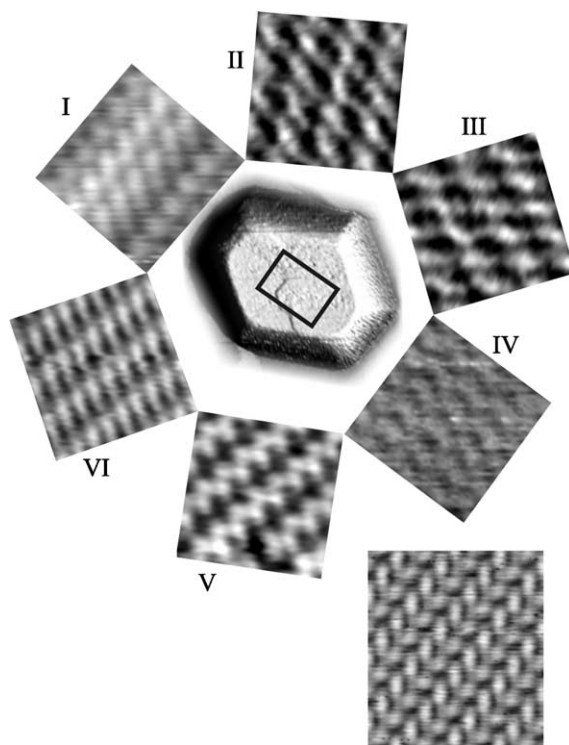
However, in general there is a displacement between the layers. Since the layers are not 'transparent' for the STM this may not be accessed directly. The displacement is visible on the slopes because the directions of the base vectors and the corresponding lines on the slopes differ significantly, as one may see e.g. in Fig. 12 for the crystallite F. The line from the lower left to the upper right is parallel to the short side of the unit cell within the top layer. The two other lines connect molecules in equivalent positions on the slopes. Using this information the displacement vector between adjacent layers may be evaluated by simple geometric triangulation. The basic scheme is displayed in Fig. 13 for the crystallite F. Since the slopes are formed by additional molecular rows, the origin of the unit cell of the next lower layer may be determined by intersecting the

Table 1
Roundup of the experimental data

Label		A	B	C	D	E	F
Figure		4	5	6	7	8	9
Substrate		Cu(1 1 0)	Cu(1 1 0)	Cu(1 1 0)	Cu(1 1 1)	Cu(1 1 1)	Au(1 1 1)
a [Å]		13.2 ± 0.8	13.7 ± 0.8	12.5 ± 0.8	12.2 ± 0.8	13.1 ± 0.8	12.7 ± 0.8
b [Å]		21.3 ± 0.8	22.9 ± 0.8	19.5 ± 0.8	20.9 ± 0.8	20.1 ± 0.8	21.1 ± 0.8
a/b		1.61	1.66	1.56	1.71	1.53	1.66
Δa [Å]		0.8 ± 0.5	0.0 ± 0.5	2.8 ± 0.5	0.53 ± 0.5	0.3 ± 0.5	−1.8 ± 0.5
Δa/a		0.06 ± 0.05	0.00 ± 0.05	0.22 ± 0.05	0.04 ± 0.05	0.03 ± 0.05	−0.14 ± 0.05
Δb [Å]		0.2 ± 0.5	0.3 ± 0.5	2.0 ± 0.5	2.57 ± 0.5	0.9 ± 0.5	−2.1 ± 0.5
Δb/b		0.01 ± 0.03	0.02 ± 0.03	0.10 ± 0.03	0.12 ± 0.03	0.05 ± 0.03	−0.10 ± 0.03
Angle I–II		125°	122°	123°	120°	124°	121°
Angle II–III		112°	116°	114°	–	111°	120°
Angle III–IV		124°	122°	123°	–	124°	119°
Angle IV–V		122°	124°	123°	–	124°	121°
Angle V–VI		113°	114°	114°	119°	111°	120°
Angle VI–I		124°	120°	123°	120°	124°	121°
Angle slope I		58°	58°	74°	–	57°	60°
Angle slope II		1°	2°	11°	12°	4°	9°
Angle slope III		1°	1°	11°	–	–	8°
Angle slope IV		53°	–	65°	–	–	63°
Angle slope V		1°	3°	7°	12°	0°	11°
Angle slope VI		2°	1°	7°	11°	–	11°

Columns display the different crystallites which have been found, the rows represent the geometrical data extracted from the STM images, the crystallites A and B show no displacement of the layers within the experimental errors, crystal D has a significant shift only along the long side of the unit cell whereas all other crystallites exhibit displacements along both directions given by the unit cell.

lines of Fig. 12 if one accounts for the additional translation. This may be done by displacing the starting point of the lines by the corresponding number of base vectors. For the angle of 8° this 'extra' displacement is given by one unit vector in the direction of the short axis of the unit cell. In principle two lines which are not parallel would be sufficient to determine the displacement. In practice the displacement between the layers can only be well defined if the lines intersect at about 90°.
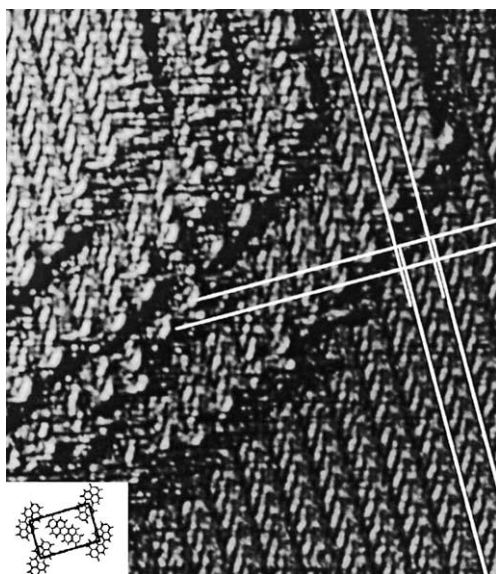
Fig. 10. Small area (about 30×33 nm^2) of the top layer of crystallite D, four monomolecular steps are visible, the white lines are parallel to the axes of the unit cell, the displacement of about $\Delta b = 2$ Å along the long side may be recognized.
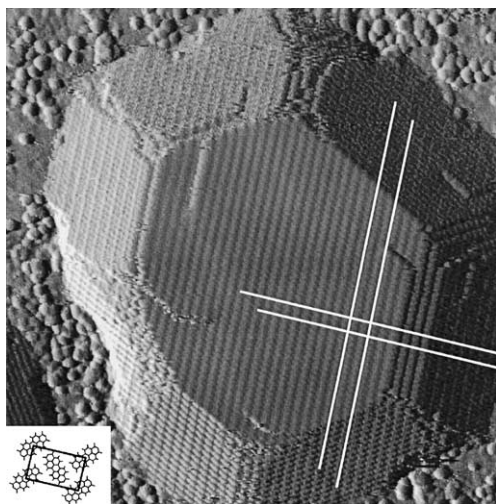

Fig. 11. Molecular resolved image of crystallite A, the white lines are parallel to the axes of the unit cell, it is apparent that these lines continue on the slopes indicating that there is no displacement between the layers.

For most crystals up to six lines may be drawn confirming the correct identification of the 'extra' displacement. A minor difficulty arises for the
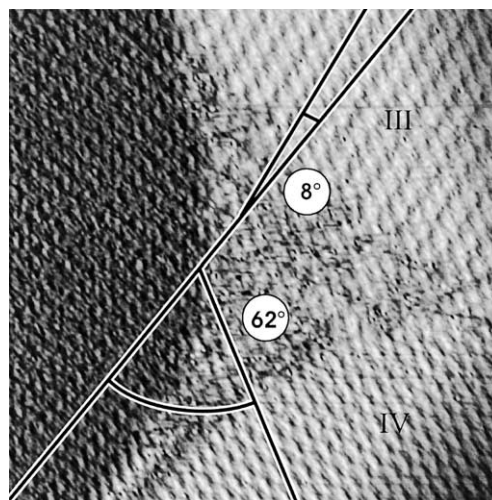
Fig. 12. Detail of crystallite F showing the top layer and the slopes III and IV, the area is 38×38 nm, $U_{tip} = -3.3$ V, $I_t = 1.2$ pA, the line from the lower left to the upper right is parallel to the short side of the unit cell of the top layer, the two other lines connect molecules in equivalent positions on the slopes.

Fig. 13. Triangulation to evaluate the shift between adjacent layers, the gray area corresponds to the unit cell of the top layer, the straight lines correspond to characteristic lines on the slopes of crystal F (see Figs. 9 and 13), the contours lines represent equal χ^2 to give an estimate of the uncertainty of the origin of the displaced unit cell.

slopes I and IV where the edges are parallel to the short axis of the unit cell. By going down one step only half of a unit cell is added in the direction of the long axis. This is readily understood by 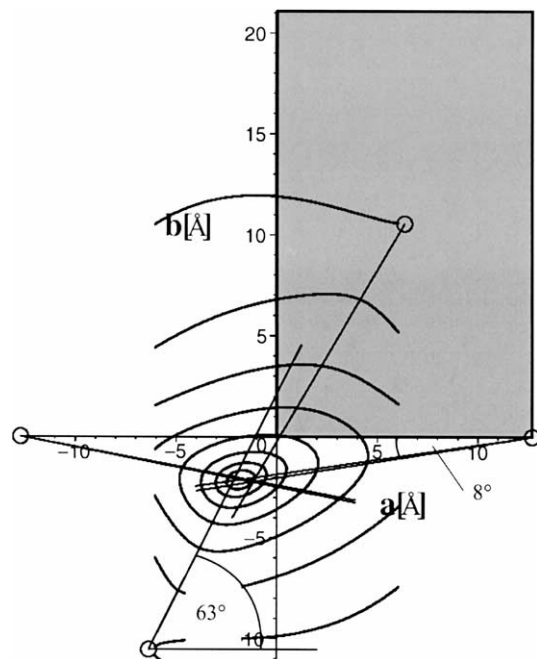looking at the unit cell of the PTCDA layer, which contains two molecules (see Figs. 10 and 11). If the origin of the unit cell is chosen at the center of one molecule the second molecule is located in the middle of the unit cell, hence it is displaced by half a unit vector in each direction. In consequence the slopes I and IV are formed by alternating rows of molecules pointing in the one or the other direction as can be seen clearly in the STM images. When implementing the information in the construction of Fig. 13 this has to be accounted for by a displacement of half a unit vector in both directions for the slopes I and IV.

For a better quantification of the uncertainty of this procedure the contour lines of χ^2 are plotted as function of the displacement vector (χ^2 is defined by the angular deviations). It can be seen that the minimum is a little shallower in the *a*-direction than the *b*-direction. The uncertainty resulting from the triangulation is typically 0.25 Å if five or more directions are included. However, this is lower than systematic errors which may be caused by the tube scanner of the STM. We estimate the latter to about 0.5 Å.

Table 1 summarizes the findings for the six crystals shown in Figs. 4–9. Within the experimental uncertainties four different types of PTCDA crystals have been found. On the one hand crystals A and B have no displacement between the layers. On the other hand crystal D exhibits a displacement of $\Delta b = 2.6$ Å along the long side of the unit cell and none along the other, hence it may be identified as α-type crystal. Compared to the lateral displacement measured by using a monomolecular step the values agree well within the experimental errors. The three remaining crystals have non-vanishing displacements Δa and Δb in both directions of the unit cell. According to crystal F it should be noted that there is a major difference to the findings of Chizov et al. [10]. Since there only a lateral displacement parallel to *b* is found the analyzed crystal F shows a displacement in both unit cell directions. This is probably a result of the different coverages and annealing conditions, since the initial layers undergo a stronger interaction to the underlying surface. Due to the investigated crystals on the Cu(1 1 0) and Cu(1 1 1) surfaces this difference is not astonishing because it is shown that different crystal structures coexist on the very same sample.

4. Summary

The example of the growth of PTCDA films shows that for particular samples scanning probe microscopy may be successfully applied to analyze the three-dimensional structure of crystals. In contrast to other methods integrating over larger areas it may be used to investigate individually very small crystallites even if many crystals with different size, structure and orientation are present.

If the molecular layers are prepared by deposition of the molecules at room temperature followed by thermal annealing, PTCDA exhibits Stranski–Krastanov growth on the metallic substrates Cu(1 1 0), Cu(1 1 1) and Au(1 1 1). While this is undesirable for most applications it offers the opportunity to analyze the crystalline structure of the initial phase of growth ranging from a few to up to 100 molecular layers for individual crystals. Our findings reveal that even for one substrate and one preparation a variety of crystals may be found indicating that there is only very little energetic difference between the different crystalline forms.

All crystals have in common a layered structure with layers parallel to the substrate. These layers resemble the (1 0 2) plane of the bulk phase of PTCDA (either α or β phase). The molecular arrangement within the layer is commonly named 'herringbone-structure'. There are two molecules within the rectangular unit cell. This structure apparently leads to the formation of well defined step edges either parallel to the short side or the diagonals of the unit cell. In consequence the crystals have a hexagonal shape.

The crystals differ slightly in the ratio between the long and the short side of the unit cell. However the major difference is the stacking of the subsequent layers. For two crystals there is no

displacement between the layers in a vertical projection. One crystal agrees with the α-phase of the bulk. The remaining three crystals exhibit a displacement along the short and the long axis of the unit cell.

References

[1] B. Uder, C. Ludwig, J. Petersen, B. Gompf, W. Eisenmenger, Z. Phys. B 97 (1995) 389.

[2] T. Schmitz-Hübsch, T. Fritz, F. Sellam, R. Staub, K. Leo, Phys. Rev. B 55 (1996) 7972.

[3] C. Kendrick, A. Kahn, S.R. Forrest, Appl. Surf. Sci. 104 (1996) 586.

[4] C. Seidel, C. Awater, X.D. Liu, R. Ellerbrake, H. Fuchs, Surf. Sci. 371 (1997) 123.

[5] K. Glöckler, C. Seidel, A. Soukupp, M. Sokolowski, E. Umbach, M. Böhringer, R. Berndt, W.-D. Schneider, Surf. Sci. 405 (1998) 1.

[6] T. Schmitz-Hübsch, T. Fritz, R. Staub, A. Back, N.R. Armstrong, K. Leo, Surf. Sci. 437 (1999) 163.

[7] E. Umbach, K. Glöckler, M. Sokolowski, Surf. Sci. 402 (1998) 20–31.

[8] T. Schmitz-Hübsch, F. Sellam, R. Staub, M. Törker, T. Fritz, Ch. Kübel, K. Müllen, K. Leo, Surf. Sci. 445 (2000) 358.

[9] R. Staub, M. Toerker, T. Fritz, T. Schmitz-Hübsch, F. Sellam, K. Leo, Surf. Sci. 445 (2000) 368.

[10] I. Chizhov, A. Kahn, G. Scoles, J. Cryst. Growth 208 (2000) 449.

[11] A.J. Lovinger, S.R. Forrest, M.L. Kaplan, P.H. Schmidt, T. Venkatesan, J. Appl. Phys. 55 (1984) 476.

[12] M. Möbus, N. Karl, T. Kobayashi, J. Cryst. Growth 116 (1992) 495.

[13] B. Krause, A.C. Dürr, K.A. Ritley, F. Schreiber, H. Dosch, D. Smilgies, Phys. Rev. B 66 (2002) 235–404.

[14] M. Stöhr, M. Gabriel, R. Möller, Europhys. Lett. 59 (2002) 423.

[15] M. Stöhr, M. Gabriel, R. Möller, Surf. Sci. 507–510 (2002) 330.